A tunnelling study on polymer/1T-Li_xTaS_2 layered nanocomposites

2004 J. Phys.: Condens. Matter 16 6375

(http://iopscience.iop.org/0953-8984/16/36/004)

INSTITUTE OF PHYSICS PUBLISHING JOURNAL OF PHYSICS: CONDENSED MATTER

J. Phys.: Condens. Matter **16** (2004) 6375–6384 PII: S0953-8984(04)79545-4

A tunnelling study on polymer/1T-Li_xTaS_2 layered nanocomposites

Hiroyuki Enomoto[1,2], **Hiroyuki Takai**[2], **Hajime Ozaki**[3] **and Michael M Lerner**[4]

[1] Academic Frontier Promotion Centre, Osaka Electro-Communication University, Hatsu-cho 18-8, Neyagawa, Osaka 572-8530, Japan
[2] Department of Materials Science, Osaka Electro-Communication University, Hatsu-cho 18-8, Neyagawa, Osaka 572-8530, Japan
[3] Department of Electrical Engineering Bioscience, Waseda University, Ohkubo 3-4-1, Shinjuku-ku, Tokyo 169-8555, Japan
[4] Department of Chemistry, Oregon State University, Corvallis 97331-4003, USA

E-mail: h-enomot@isc.osakac.ac.jp

Received 19 April 2004
Published 27 August 2004
Online at stacks.iop.org/JPhysCM/16/6375
doi:10.1088/0953-8984/16/36/004

Abstract

Electronic structures near the Fermi level of polymer/1T-Li_xTaS_2 layered nanocomposites have been studied by tunnelling spectroscopy. Polymer/1T-Li_xTaS_2 layered nanocomposites were synthesized by using the exfoliation–adsorption technique. Single crystals of 1T-TaS_2 were used as host materials. Poly(ethylene oxide) (PEO) and poly(ethylenimine) (PEI) with different molecular weights were adopted as guest intercalants. Powder x-ray diffraction patterns showed that all samples of the polymer/1T-Li_xTaS_2 layered nanocomposites contain organic polymer between all individual 1T-TaS_2 sheets. Although 1T-TaS_2 single crystal is well known to show quite unique temperature dependences of the resistivity due to the charge density wave (CDW), the resistivities of all polymer/1T-Li_xTaS_2 nanocomposites showed semiconductor-like temperature dependences. The tunnelling spectra of polymer/1T-Li_xTaS_2 nanocomposites revealed that the CDW gap disappears in the density of states near the Fermi level of polymer/1T-Li_xTaS_2 nanocomposites and their electronic structures show a metallic behaviour.

1. Introduction

Layered materials are characterized by strongly bound sheets with weaker interactions along the stacking direction. Early studies on layered materials primarily involved the intercalation of simple, small ions into the van der Waals gap [1–3]. Recently, a new class of these materials

has been developed based on an extension of these concepts, involving the incorporation of macromolecular species, such as organic polymers, between the layers.

Many transition metal dichalcogenides MX_2 have layered crystal structures, with transition metal atoms M sandwiched between hexagonally packed chalcogen layers X. The transition metals may be coordinated octahedrally, as in the case of 1T-TaS_2, or trigonal-prismatically, as in 2H-TaS_2. These polytypes of 1T- and 2H-TaS_2 have peculiar charge density waves (CDWs), resulting from the quasi-two-dimensional natures of their Fermi surfaces [4, 5]. MX_2 are known to allow intercalation reactions with alkalis, alkaline earths, transition metals, and a number of organic and inorganic compounds of the Lewis base type [1, 2]. The intercalation of nitrogen donors into TaS_2 had been widely studied. This marked the beginning of the intercalation chemistry of MX_2 in the 1970s, because the discovery of superconductivity in the intercalation compounds of MX_2 began a very wide investigation of these compounds [3]. The discovery of the exfoliation of MoS_2 into monolayers [6] has enabled a new synthetic route to numerous nanocomposites of layered MX_2 with organic polymers. The exfoliation–adsorption technique is an attractive method when the host material can be delaminated into a single-sheet colloid and the polymer is soluble [7–17].

Structures of the intercalated polymers in nanocomposites have gained increasing interest. For example, the polymer arrangement in the gallery can be precisely analysed using one-dimensional electron density maps calculated from x-ray diffraction data [18]. Spectroscopic studies, such as infrared (IR) spectroscopy and x-ray photoemission spectroscopy (XPS or ESCA), have been also carried out to determine the structures of nanocomposites [7–11, 19–23]. Wang *et al* had prepared layered nanocomposites of PEO, PEI, and PVP with 2H-Li_xTaS_2, and had examined the structure of the intercalated PEO polymers in the gallery of TaS_2 sheets [24]. However, few studies have been reported on the electronic band structures of nanocomposites.

Tunnelling spectroscopy is a powerful tool for investigating the energy band structures of conductive materials near the Fermi level, because the first-derivative curve of the tunnelling current across the tunnel junction is basically proportional to the density of states (DOS) [25–35]. Recently, we have synthesized layered nanocomposites of 1T-TaS_2 [13–15], 2H-TaS_2 [15, 16] and 4Hb-TaS_2 [17] by using the exfoliation–adsorption technique. In this paper, we report on the electronic structures of polymer/1T-Li_xTaS_2 layered nanocomposites using tunnelling spectroscopy.

2. Experimental details

2.1. Sample preparation

TaS_2 host crystals were prepared by the chemical vapour transport method with the use of the I_2 agent [27, 28, 32]. Ta powder (99.96%, Rare Metallic Co.) and S powder (99.99%, Rare Metallic Co.) in stoichiometric amounts were sealed in a quartz ampoule (diameter 11×200 mm) under a vacuum of $<5 \times 10^{-4}$ Pa. After 24 h at 1050 °C, for complete reaction of tantalum with sulfur, the ampoule was kept at 920 °C for 92 h to grow polycrystalline TaS_2. TaS_2 polycrystalline powder was resealed into a quartz ampoule with excess S and the transfer agent I_2. Single crystals of 1T-TaS_2 were obtained after growth at 950 °C for 149 h with rapid quenching into cold water. Before lithiation, the purity and identity of each powder was confirmed by means of x-ray powder diffraction and the temperature dependence of the resistivity.

1T-Li_xTaS_2 was prepared by the reaction of 1T-TaS_2 single-crystal powders with three times the molar ratio of *n*-butyllithium (BuLi, 1.6 M in hexane, Aldrich) at room temperature for five days, carried out under dry N_2 gas atmosphere in a glove box (Miwa Seisakusho Co., MDB-1B-O). The product was filtered, washed with hexane, and then dried *in vacuo* overnight.

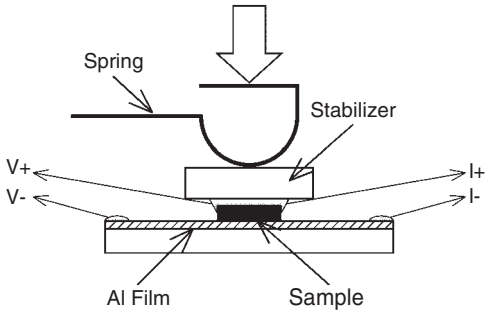

Figure 1. A planar contact tunnel junction.

Polymer/1T-Li_xTaS_2 nanocomposites were synthesized by the exfoliation–adsorption method [13–17]. In typical reactions, 0.5 g of 1T-Li_xTaS_2 was exfoliated by ultrasonication for 30 min at ambient temperature in 20 ml of distilled, deionized, and deaerated (DI/DA) water. Poly(ethylene oxide) (PEO, $M_v \sim 100\,000$, Aldrich), poly(ethylene glycol) (PEG, $M_v \sim 10\,000$, Aldrich), poly(ethylenimine) (PEI, $M_w \sim 750\,000$, Aldrich) and low molecular weight PEI (LPEI, $M_w \sim 25\,000$, Aldrich) were used as received. An aqueous solution containing excess polymer (0.5 g) with 20 ml of DI/DA water was slowly dropped into the colloid suspension containing TaS_2 single sheets. The mixtures were stirred for a controlled time. A precipitate was obtained by acidifying the solution. The nanocomposites were then collected by centrifugation, washed several times with small amounts of DI/DA water, and dried *in vacuo* overnight.

X-ray powder diffraction (XRD) data were collected on a Rigaku RINT Ultima$^+$ diffractometer by the use of the fundamental parameter approach with the Bragg–Brentano reflection geometry, using Ni-filtered Cu Kα radiation. The electrical DC resistivity ρ_{DC} was measured by the standard van der Pauw method [36, 37]. A powdered sample was pressed into a pellet 13 mm in diameter. Ag paste was painted on the sample surface to form an electrode, and was quickly dried to prevent chemical reaction with the sample. The temperature dependence of the electrical resistivity between 300 and 10 K was measured using a closed-cycle helium refrigerator (Iwatani Gas, CRT-105-RE). Impedance spectroscopy was performed from 300 to 10 K in the frequency range between 42 Hz and 5 MHz using an LCR multimeter (HIOKI, 3532-50).

2.2. Tunnelling spectroscopy

All tunnelling spectroscopy measurements in this paper were performed at room temperature. The tunnel junction was fabricated using the planar contact technique [29–31]. Figure 1 shows a tunnel junction fabrication. An Al film 10 μm thick was evaporated onto a chemically cleaned surface of a micro-slide glass under a vacuum of 5×10^{-4} Pa. After the vacuum evaporation, the Al film surface was oxidized in an O_2 atmosphere for 20 min. The thickness of the oxide layer was estimated to be about 5 nm. The pelletized sample surface was softly pressed onto the surface of the Al_2O_3/Al plate by using a phosphor–bronze spring. A stabilizer on the sample was used to transfer the pressure from the spring uniformly to the tunnel junction.

Tunnelling measurements were performed using the standard AC modulation technique. In this study, the modulation bias was 6.9 mV (RMS) and the modulation frequency was 1 kHz.

3. Results and discussion

Figure 2 shows the XRD patterns of polymer/1T-Li_xTaS_2 nanocomposites. The results for optimal reaction times are summarized in table 1, together with the synthesis conditions, the

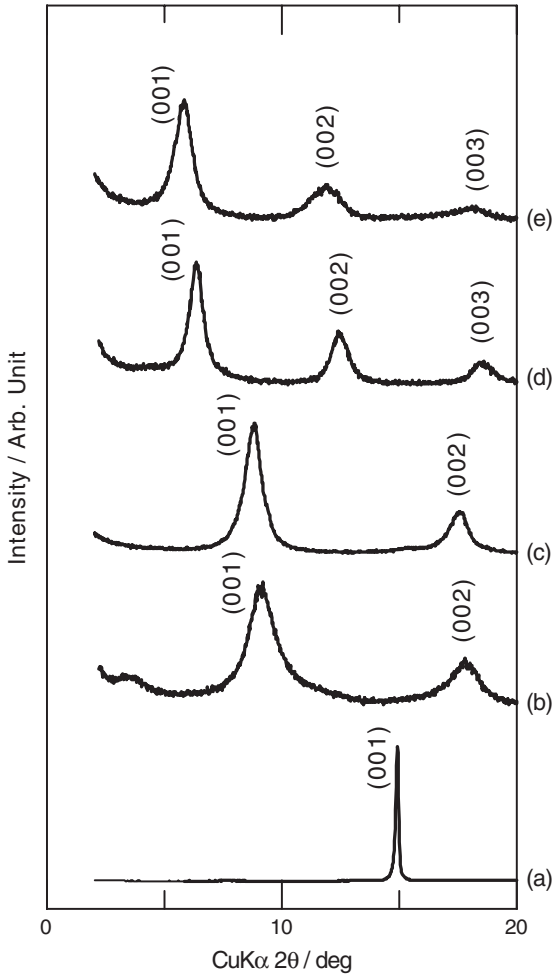

Figure 2. XRD patterns of the host and its nanocomposites; (a) 1T-TaS_2 single crystal, (b) LPEI/1T-Li_xTaS_2 nanocomposite, (c) PEI/1T-Li_xTaS_2 nanocomposite, (d) PEG/1T-Li_xTaS_2 nanocomposite, and (e) PEO/1T-Li_xTaS_2 nanocomposite.

Table 1. Synthesis conditions and XRD data for polymer/1T-Li_xTaS_2 layered nanocomposites. t: reaction time, d: interlayer spacing, Δd: the difference between interlayer spacing of nanocomposite and unintercalated layered host, L_c: crystalline size estimated by using Scherrer's equation from the (001) diffraction peak, and $\rho_{300\ K}$: electrical DC resistivity at 300 K.

Sample	t (h)	d (nm)	Δd (nm)	L_c (nm)	$\rho_{300\ K}$ (Ω cm)
1T-TaS_2	—	0.59	—	69	7.1×10^{-4}
LPEI/1T-Li_xTaS_2	18	0.97	0.38	9	8.2×10^{-1}
PEI/1T-Li_xTaS_2	18	1.00	0.41	13	2.7×10^{0}
PEG/1T-Li_xTaS_2	23	1.40	0.81	17	2.1×10^{-1}
PEO/1T-Li_xTaS_2	24	1.54	0.95	15	2.1×10^{0}

crystalline size L_c perpendicular to the basal plane of the nanocomposite obtained from the x-ray line broadening by using Scherrer's equation [38–40], and the electrical DC resistivity $\rho_{300\ K}$ at 300 K. To estimate L_c, the line broadening was obtained by fitting the Gaussian

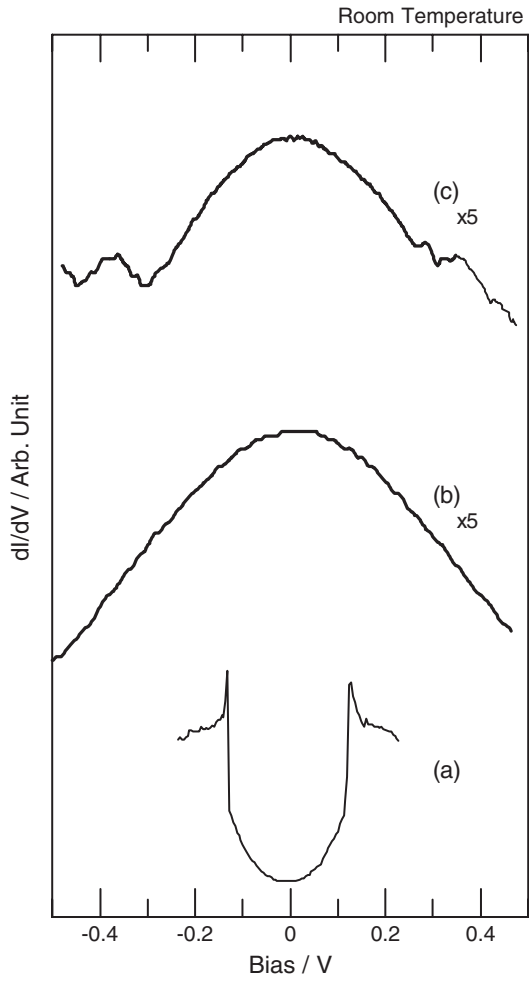

Figure 3. Tunnelling spectra measured at room temperature; (a) 1T-TaS_2 single crystal, (b) PEI/1T-Li_xTaS_2 nanocomposite, and (c) PEO/1T-Li_xTaS_2 nanocomposite.

distribution function after background removal. All single-phase polymer/1T-Li_xTaS_2 nanocomposites have no XRD diffraction peaks of their host at 14.7°, indicating that polymer is present between all the individual 1T-TaS_2 sheets. The basal plane expansions $\Delta d = 0.38$–0.41 nm for PEI/1T-Li_xTaS_2 and LPEI/1T-Li_xTaS_2 nanocomposites are consistent with the values for reported PEI-containing nanocomposites (0.38–0.47 nm) [9, 13–16] for incorporation of a PEI monolayer into host galleries. The basal plane expansions $\Delta d = 0.81$–0.95 nm for PEO/1T-Li_xTaS_2 and PEG/1T-Li_xTaS_2 nanocomposites are in good agreement with the values for reported PEO-containing nanocomposites (0.81–0.94 nm) [7–11, 13–17] for a PEO or PEG bilayer intercalate. Here, PEO and PEG are the same material with the same chemical formula but with different molecular weight. Lower molecular weight PEO is commonly known as PEG. The observation of only (00*l*) diffraction peaks indicates that these nanocomposites have layered structures, and are highly oriented along the *c*-direction.

Figure 3 shows the tunnelling spectra of polymer/1T-Li_xTaS_2 nanocomposites measured at room temperature. The positive bias side corresponds to the conduction band side

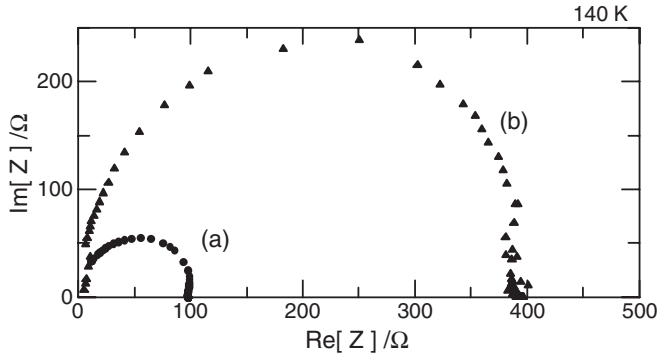

Figure 4. Impedance spectra measured at 140 K; (a) PEO/1T-Li_xTaS_2 nanocomposite and (b) PEI/1T-Li_xTaS_2 nanocomposite.

of the nanocomposite. The tunnelling spectrum of 1T-TaS_2 single crystal, as shown in figure 3(a), shows a clear CDW gap of about 0.26 eV, which is consistent with the reported value [27, 28]. The CDW gap disappears in the tunnelling spectra of both PEO/1T-Li_xTaS_2 and PEI/1T-Li_xTaS_2 nanocomposites, as shown in figures 2(b) and (c). Although the intensities of the tunnelling spectra of polymer/1T-Li_xTaS_2 nanocomposites are lower than those for 1T-TaS_2 single crystal and other normal metals, the electronic structures of polymer/1T-Li_xTaS_2 nanocomposites near the Fermi level are found to show a metallic behaviour.

Figure 4 shows the impedance spectra of PEI/1T-Li_xTaS_2 and PEO/1T-Li_xTaS_2 nanocomposites at 140 K, as an example. In the temperature range measured, the samples show similar impedance spectra. Both PEI and PEO are well known to form ionically conducting polymer–salt complexes, so an ionic contribution to the overall conductivities reported here should be considered. For a mixed conductor where two conduction mechanisms have very different dielectric relaxation times, impedance spectra can resolve these mechanisms. However, the impedance spectra of both PEI/1T-Li_xTaS_2 and PEO/1T-Li_xTaS_2 nanocomposites all show only a single semicircle in the frequency range measured, as shown in figure 4. In addition, ionic conduction is not expected to contribute significantly to the high conductivity values observed at a low temperature such as 140 K. For these reasons, the contribution of ionic conductivity is considered negligible in these analyses.

The temperature dependences of the electrical DC resistivity, ρ_{DC}, and AC resistivity, ρ_{AC}, of pelletized polymer/1T-Li_xTaS_2 nanocomposites are shown in figure 5. All resistivities of polymer/1T-Li_xTaS_2 layered nanocomposites at room temperature are several orders higher than that of 1T-TaS_2 single crystal. Although 1T-TaS_2 single crystal shows peculiar CDW transitions, as shown in figure 5(a), no CDW transition can be observed in the ρ–T curve for all polymer/1T-Li_xTaS_2 nanocomposites in the temperature range measured, which is consistent with the non-CDW-gap DOS structures observed in the tunnelling spectra of these nanocomposites, as shown in figure 3. Polymer/1T-Li_xTaS_2 nanocomposites show a semiconductor-like dependence at lower temperatures. $\rho_{300\ K}$ of PEI/1T-Li_xTaS_2 nanocomposite is higher than that of PEO/1T-Li_xTaS_2, while the basal plane expansion of PEI/1T-Li_xTaS_2 nanocomposite ($\Delta d \sim 0.4$ nm) is smaller than that of PEO/1T-Li_xTaS_2 ($\Delta d \sim 0.9$ nm), as shown in table 1. $\rho_{300\ K}$ of PEI/1T-Li_xTaS_2 nanocomposite is higher than that of LPEI/1T-Li_xTaS_2, while the basal separations of PEI/1T-Li_xTaS_2 and LPEI/1T-Li_xTaS_2 nanocomposites are almost same. The ρ–T curve of PEO/1T-Li_xTaS_2 nanocomposite is almost one order higher than that of PEG/1T-Li_xTaS_2, while the basal separation of PEO/1T-Li_xTaS_2 nanocomposite is almost same as that of PEG/1T-Li_xTaS_2. This is because the polymers have

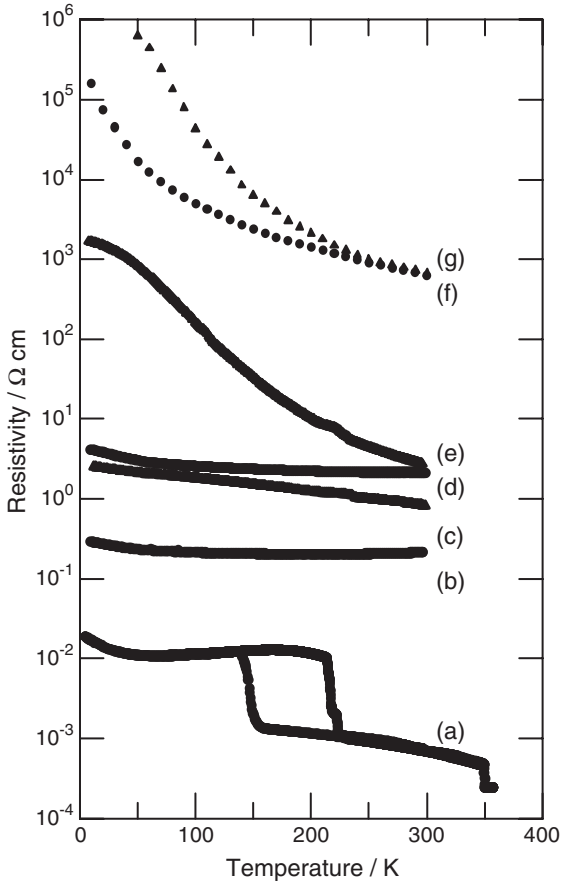

Figure 5. Temperature dependences of the electrical resistivities; (a) ρ_{DC} of 1T-TaS_2 single crystal, (b) ρ_{DC} of PEG/1T-Li_xTaS_2 nanocomposite, (c) ρ_{DC} of LPEI/1T-Li_xTaS_2 nanocomposite, (d) ρ_{DC} of PEO/1T-Li_xTaS_2 nanocomposite, (e) ρ_{DC} of PEI/1T-Li_xTaS_2 nanocomposite, (f) ρ_{AC} of PEO/1T-Li_xTaS_2 nanocomposite, and (g) ρ_{AC} of PEI/1T-Li_xTaS_2 nanocomposite.

different charges and will have different interactions with the negatively charged host. Due to the different electrode geometries and the preferred orientation of particles in the sample pellets, the DC data measure the resistivity parallel to the host layers of the nanocomposites, while the AC data indicate the resistivity perpendicular to these layers. The differences between curves (f) and (d) in figure 5 and curves (g) and (e) in figure 5 represent the anisotropies of these layered nanocomposites.

Since polymer/1T-Li_xTaS_2 layered nanocomposites show semiconductor-like temperature dependences, as shown in figure 5, the variable range hopping (VRH) conduction model is considered as a transport mechanism in the polymer/1T-Li_xTaS_2 layered nanocomposite [14, 15]. The electrical resistivity ρ is given by Mott's law [41, 42],

$$\rho(T) = \rho_0 \exp\left[\left(\frac{T_0}{T}\right)^{\frac{1}{d+1}}\right], \tag{1}$$

where ρ_0 may be a virtually temperature independent material parameter, T_0 can be interpreted as an effective energy separation between localized states, and d is the dimensionality of the

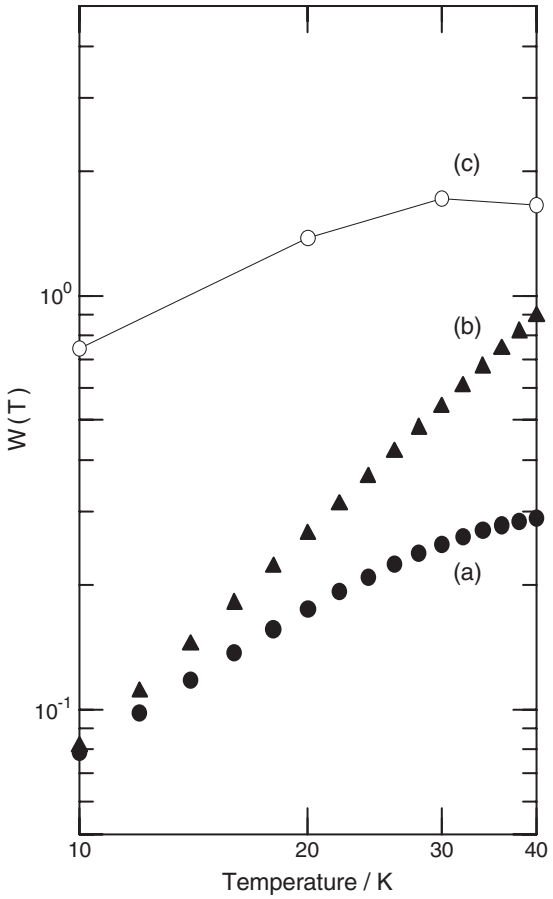

Figure 6. Log–log plots of W versus T; (a) ρ_{DC} for PEO/1T-Li_xTaS_2 nanocomposite, (b) ρ_{DC} for PEI/1T-Li_xTaS_2 nanocomposite, and (c) ρ_{AC} for PEO/1T-Li_xTaS_2 nanocomposite.

hopping conduction. In contrast to experimental results of a clear $T^{-1/4}$ dependence of $\log \rho$ in PEI/Li_xMoS_2 nanocomposite [14] and the $T^{-1/3}$ dependence in N_2H_4/1T-TaS_2 [43], all samples may have straight-line regions in $\log \rho$ against $T^{-1/2}$, $T^{-1/3}$, and $T^{-1/4}$. It is very difficult to decide the dimensionality of polymer/1T-Li_xTaS_2 nanocomposites from the plots of $\log \rho$ against $T^{-1/n}$.

To decide the dimensionality more precisely, the reduced activation energy is introduced as a logarithmic derivative of $\rho(T)$ [44–48]:

$$W(T) = -\frac{\mathrm{d} \ln \rho(T)}{\mathrm{d} \ln T}. \tag{2}$$

$1/(d+1)$ can be then determined directly from the slope of the plot of $\ln W(T)$ versus $\ln T$ which is normally found to be a straight line:

$$\ln W(T) = \left[\frac{1}{d+1} \ln T_0 + \ln\left(\frac{1}{d+1}\right)\right] - \frac{1}{d+1} \ln T. \tag{3}$$

Figure 6 shows the log–log plots of W–T for polymer/1T-Li_xTaS_2 nanocomposites. A linear relationship with a positive slope can be observed in figure 6. This positive slope of W–T plots represents the system being still in the metallic region of the metal–insulator transition. This

result is consistent with the metallic behaviour in the tunnelling spectra of figure 3. Together with the results from tunnelling spectra, ρ–T curves, and W–T plots, it is considered as showing that the Fermi level of polymer/1T-Li_xTaS_2 nanocomposite locates not in the bandgap but in the band, which results in the metallic behaviour of the tunnelling spectra and W–T plots. And it is also considered that there exist localized states at the Fermi level in polymer/1T-Li_xTaS_2 nanocomposite, which causes a semiconductor-like ρ–T curve. As the electron transfer occurs in the Li-ion intercalation into the TaS_2 host [49, 50], the Li-ion content x should be checked before/after syntheses of polymer/1T-Li_xTaS_2 nanocomposites. Further experiments, such as the temperature dependent tunnelling spectroscopy of Li-ion controlled polymer/1T-Li_xTaS_2 nanocomposites, are needed to reveal the electronic structure of polymer/1T-Li_xTaS_2 layered nanocomposites in more detail.

4. Summary

Various polymer/1T-Li_xTaS_2 layered nanocomposites have been synthesized by using the exfoliation–adsorption technique. Single phases of PEI/1T-, LPEI/1T-, PEO/1T-, and PEG/1T-Li_xTaS_2 layered nanocomposites are synthesized. Although 1T-TaS_2 single crystals show quite different temperature dependences of the resistivity due to the CDW, the resistivities of all nanocomposites show semiconductor-like temperature dependences at lower temperature. The tunnelling spectra of polymer/1T-Li_xTaS_2 nanocomposites reveal that the electronic structure of nanocomposite near the Fermi level has a metal-like DOS structure at room temperature.

Acknowledgments

The authors gratefully acknowledge Miss Yuka Nakajima and Mr Makoto Kumagai for their kind help in sample preparations and characterizations. And the authors would like to thank Professor Masayuki Kawaguchi of Osaka Electro-Communication University for helpful discussions.

References

[1] Jacobson A J and Wittingham M S 1982 *Intercalation Chemistry* (New York: Academic)
[2] Bruce D W and O'Hare D 1992 *Inorganic Materials* (New York: Wiley)
[3] Lerf A 2000 *Handbook of Nanostructured Materials and Nanotechnology* vol 5, ed N S Nalwa (New York: Academic) p 1
[4] Wilson J A and Yoffe A D 1969 *Adv. Phys.* **18** 193
[5] Wilson J A, Di Salvo F J and Mahajan S 1975 *Adv. Phys.* **24** 117
[6] Joenson P, Frindt R F and Morrison S R 1986 *Mater. Res. Bull.* **21** 457
[7] Lemmon J P and Lerner M M 1994 *Chem. Mater.* **6** 207
[8] Lemmon J P and Lerner M M 1995 *Solid State Commun.* **94** 533
[9] Oriakhi C O, Nafshun R L and Lerner M M 1996 *Mater. Res. Bull.* **31** 1513
[10] Oriakhi C O and Lerner M M 1996 *Chem. Mater.* **8** 2016
[11] Oriakhi C O and Lerner M M 1996 *Mater. Res. Soc. Symp. Proc.* **435** 495
[12] Lerner M M and Oriakhi C O 1997 *Handbook of Nanophase Materials* ed A N Goldstein (New York: Dekker) p 199
[13] Enomoto H and Lerner M M 2002 *Mater. Res. Bull.* **37** 1499
[14] Enomoto H, Kawaguchi M, Sukpirom N and Lerner M M 2002 *Proc. SPIE* **4810** 99
[15] Enomoto H, Kawaguchi M and Lerner M M 2003 *Proc. SPIE* **5223** 241
[16] Enomoto H and Lerner M M 2004 *J. Phys. Chem. Solids* **65** 587
[17] Enomoto H and Lerner M M 2004 *Solid State Commun.* **129** 157

[18] Wang L, Rocci-Lane M, Brazis P, Kannewurf C R, Kim Y-I, Lee W, Choy J-H and Kanatzidis M G 2000 *J. Am. Chem. Soc.* **122** 6629
[19] Sukpirom N, Oriakhi C O and Lerner M M 2000 *Mater. Res. Bull.* **35** 325
[20] Kanatzidis M G, Bissessur R, DeGroot D C, Schindler J L and Kannewurf C R 1993 *Chem. Mater.* **5** 595
[21] Wang L, Schindler J, Thomas I A, Kannewurf C R and Kanatzidis M G 1995 *Chem. Mater.* **7** 1753
[22] González G, Santa Ana M A and Benavente E 1997 *J. Phys. Chem. Solids* **58** 1457
[23] Harris D J, Bonagamba T J and Schmidt-Rohr K 1999 *Macromolecules* **32** 6718
[24] Wang L and Kanatzidis M G 2001 *Chem. Mater.* **13** 3717
[25] Esaki L 1966 *J. Phys. Soc. Japan* **21** (Suppl.) 589
[26] Burstein E and Lundqvist S 1969 *Tunnelling Phenomena in Solids* (New York: Plenum)
[27] Ozaki H, Mutoh T, Ohshima H, Okubora A and Yamagata N 1983 *Physica* B **117/118** 590
[28] Ozaki H, Ohara T, Fujimoto H and Hotch H 1985 *Charge Density Waves in Solids* ed H Arai *et al* (Tokyo: Springer) p 141
[29] Enomoto H, Gotoh K, Iida K, Takano Y, Mori N and Ozaki H 1988 *Mater. Res. Soc. Symp. Proc.* **99** 853
[30] Miyamoto Y, Enomoto H and Ozaki H 1989 *J. Phys. Soc. Japan* **58** 2092
[31] Enomoto H and Ozaki H 1991 *J. Phys.: Condens. Matter* **3** 3265
[32] Enomoto H, Ozaki H, Suzuki M, Fujii T and Yamaguchi M 1991 *J. Vac. Sci. Technol.* B **9** 1022
[33] Shiikuma K, Ezaki T, Enomoto H and Ozaki H 1992 *Science and Technology of Mesoscopic Structures* ed S Namba, C Hamaguchi and T Ando (Tokyo: Springer) p 292
[34] Enomoto H, Kokado H, Matsubara I, Mori N and Ozaki H 1996 *Czech. J. Phys.* **46** (Suppl. S3) 1331
[35] Morikawa K, Enomoto H, Matsubara I, Mori N and Ozaki H 1999 *Appl. Surf. Sci.* **144/145** 534
[36] van der Pauw L J 1958 *Philips Res. Rep.* **13** 1
[37] Ramadan A A, Gould R D and Ashour A 1994 *Thin Solids Films* **239** 272
[38] Klug H P and Alexander L E 1974 *X-ray Diffraction Procedures for Polycrystalline and Amorphous Materials* 2nd edn (New York: Wiley)
[39] Hammond C 1997 *The Basic Crystallography and Diffraction* (Oxford: Oxford University Press)
[40] Mittemeijer E J and Scardi P 2004 *Diffraction Analysis of the Microstructure of Materials* (New York: Springer)
[41] Mott N F and Davis E A 1979 *Electronic Processes in Non-Crystalline Materials* 2nd edn (Oxford: Clarendon)
[42] Mott N 1987 *Conduction in Non-Crystalline Materials* (Oxford: Clarendon)
[43] Yoffe A D 1990 *Solid State Ion.* **39** 1
[44] Yoon C O, Reghu M, Moses D, Heeger A J, Cao Y, Chen T-A, Wu X and Rieke R D 1995 *Synth. Met.* **75** 229
[45] Mandal S K, Gangopadhyay A, Chaudhuri S and Pal A K 1999 *Vacuum* **52** 485
[46] Mikat J, Orgzall I, Lorenz B, Sapp S, Martin C R, Burris J L and Hochheimer H D 1999 *Physica* B **265** 154
[47] Kodama K, Koshiba T, Yamato H and Wernet W 2001 *Polymer* **42** 1533
[48] Kim B H, Jung J H, Kim J W, Choi H J and Joo J 2001 *Synth. Met.* **117** 115
[49] For example, Dines M B 1975 *Mater. Res. Bull.* **10** 287
[50] Whittingham M S and Jacobson A J 1982 *Intercalation Chemistry* (New York: Academic)